Heat Transfer Regimes in Nuclear-Reactor-Pumped Gas Lasers

J. R. Torczynski*
Sandia National Laboratories, Albuquerque, New Mexico 87185

The flow induced in nuclear-reactor-pumped gas lasers by spatially nonuniform fission-fragment heating and by heat transfer to the walls is examined. The equations of motion are acoustically filtered, and the resulting equations have three time scales: the heating duration, the time over which an $\mathcal{O}(1)$ pressure rise is produced, and the thermal boundary-layer growth time. Three distinct regimes emerge from consideration of the relative magnitudes of these time scales. In the negligible-condition regime, heating nonuniformity determines the motion. In the dominant-conduction regime, thermal-conduction effects govern the motion. In the mixed regime, both effects are comparable but oppositely directed, producing a complex motion. Analytical solutions for the motion and for $\partial^2\rho/\partial x^2$ (used in optical analyses) are presented for the first two regimes, and numerical examples are given for all three.

Nomenclature

c_p = specific heat at constant pressure
c_v = specific heat at constant volume
e = energy per unit mass
G = spatial variation of applied heating
h = temporal variation of applied heating
k = thermal conductivity
k_0 = initial thermal conductivity
$\tilde{k}$ = k/k_0 (nondimensional)
L = domain semiextent in x
p = pressure
p_0 = initial pressure
$\bar{p}$ = x-averaged p
$\hat{p}$ = $p - \bar{p}$
$\tilde{p}$ = $\bar{p}/p_0$ (nondimensional)
Q = volumetric applied heating
Q_s = amplitude of applied heating
$\tilde{Q}$ = Q/Q_s (nondimensional)
R = gas constant
S_A = amplitude similarity parameter
S_B = boundary-layer similarity parameter
S_B^* = S_B value when $t_D \approx t_C$
S_F = foil-thickness similarity parameter
S_H = homogeneity similarity parameter
S_Q = heating similarity parameter
T = temperature
T_0 = initial temperature
$\tilde{T}$ = T/T_0 (nondimensional)
t = time
t_C = thermal-conduction timescale
t_D = heating duration
$\tilde{t}$ = t/t_D (nondimensional)
u = velocity x component
$\tilde{u}$ = ut_D/L (nondimensional)
x = Cartesian coordinate (across width)
$\tilde{x}$ = x/L (nondimensional)
$\tilde{x}_0$ = Lagrangian parametric variable
α = thermal conductivity exponent
γ = specific heat ratio
κ = thermal diffusivity = $k_0/\rho_0 c_v$
μ = shear viscosity
μ_0 = initial shear viscosity
$\tilde{\mu}$ = μ/μ_0 (nondimensional)
μ_v = bulk viscosity
$\tilde{\mu}_v$ = μ_v/μ_0 (nondimensional)
ξ = dummy variable
$\tilde{\pi}$ = $\hat{p}t_D^2/\rho_0 L^2(1 + S_B)$ (nondimensional)
ρ = density
ρ_0 = initial density
$\tilde{\rho}$ = ρ/ρ_0 (nondimensional)
$\partial^2\rho/\partial x^2$ = density second derivative

Received May 17, 1990; presented at the AIAA/ASME 5th Joint Thermophysics and Heat Transfer Conference, Seattle, WA, June 18–20, 1990; revision received July 23, 1990; accepted for publication July 25, 1990.

*Senior Member of the Technical Staff, Fluid and Thermal Sciences Department, Division 1512. Member AIAA.

Introduction

IT is possible to pump gas lasers with the energetic products of fission reactions (fission fragments) induced by a pulse of neutrons from a nuclear reactor.[1-10] Such nuclear-reactor-pumped lasers have some important advantages over lasers with other pumping methods. First, the nuclear energy is utilized directly to excite atomic or molecular lasing states. The alternative to this is conversion of the nuclear energy to heat and subsequently to electricity (with the associated efficiency losses at each conversion) before being used to excite the laser medium.[11] Second, these lasers can take advantage of the large energy densities associated with nuclear power.[11]

Figure 1 shows one type of a laser cell. When irradiated with the neutron flux from a nuclear reactor, coatings of fissionable material on the side walls of the laser cell emit fission fragments. Some of these fission fragments pass through the gas-filled region of the laser cell, depositing energy as they go. Since most of the deposited energy is rapidly thermalized, the pumping process heats the gas. This heating is large (the energy deposited is comparable to the thermal energy originally present), transient (the neutron flux varies temporally), spatially nonuniform (the fission fragments heat the gas more near the side walls), and volumetric (the fission fragments penetrate deeply into the gas to deposit energy). The heating nonuniformity induces gas motion in toward the center (laser optical axis). However, the side walls remain colder than the gas, so heat transfer effects induce gas motion out toward the walls. Since these effects are oppositely directed, heat transfer and heating-nonuniformity effects compete to determine the overall gas motion.

Since the density of a gas is related to its refractive index,[12] this gas motion establishes gradients in the refractive index normal to the optical axis. More specifically, the heated gas acts like a lens with a temporally varying focal length. Under certain circumstances, the lensing produced in this manner can change the optical stability of the laser resonator.[13-15] Thus, in order to predict the optical behavior of these lasers, it is essential to understand the gas motion induced by thermal conduction and heating nonuniformity.

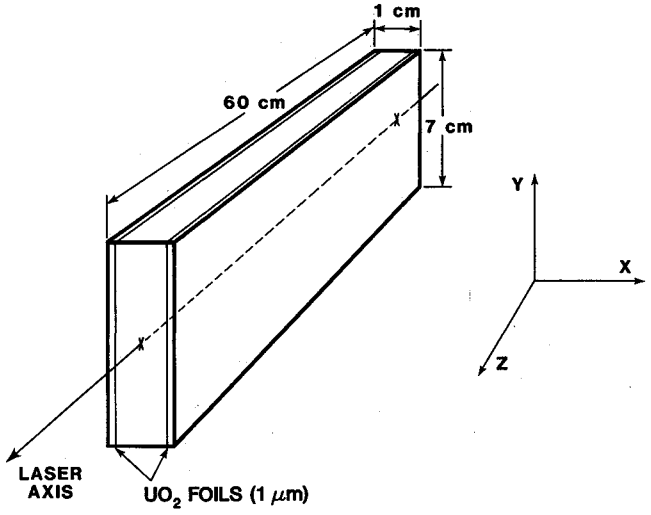

Fig. 1 Schematic diagram of a laser cell.

Previous studies have concentrated on the gas motion induced by the heating nonuniformity but have neglected thermal conduction.[16–20] Although this is justified for short pulses during which the effects of thermal conduction are confined to thin thermal boundary layers at the side walls, this assumption breaks down for longer pulses. In this paper, the gas motion in a nonuniformly heated laser medium is analyzed including the effects of heat transfer to the cold side walls. Three heat transfer regimes are found. Analytical solutions for the induced gas flow are presented for two of the regimes, and examples are presented for all three regimes.

Model Problem

The following model describing the gas motion is considered. The gas is assumed to obey the perfect gas law,

$$p = R\rho T \tag{1}$$

The gas is also assumed to have constant specific heats c_p and c_v, with the ratio $\gamma = c_p/c_v$ thus constant (for polyatomic molecules raised to high temperatures, it is necessary to relax this assumption and incorporate the temperature dependences of c_p, c_v, and γ). The thermal conductivity of the gas is assumed to vary with temperature according to the relation

$$k = k_0(T/T_0)^\alpha \tag{2}$$

where k_0, T_0, and α are constants. This relation, although approximate, provides a relatively accurate representation of the thermal conductivity of many gases.[21] Appropriate temperature dependences are also assumed for the shear and bulk viscosities although they are not important in the following analysis.

Flow and variation of thermodynamic properties are allowed only in the x direction (see Fig. 1). Thus, this model neglects variations in the y and z directions. Such variations are often minor[13,20]; moreover, the emphasis herein is on heating-nonuniformity and thermal-conduction effects, which are strongest in the x direction. The values $x = \pm L$ and $x = 0$ are chosen to correspond to the side walls and to the center plane, respectively, and symmetry about $x = 0$ is assumed henceforth.

The equations describing the gas motion are the conservation equations for mass, momentum in the x direction, and energy:

$$\frac{\partial \rho}{\partial t} + \frac{\partial}{\partial x}\rho u = 0 \tag{3}$$

$$\frac{\partial}{\partial t}\rho u + \frac{\partial}{\partial x}\rho u^2 = -\frac{\partial p}{\partial x} + \frac{\partial}{\partial x}\left[\left(\frac{4}{3}\mu + \mu_v\right)\frac{\partial u}{\partial x}\right] \tag{4}$$

$$\frac{\partial}{\partial t}\rho\left(e + \frac{1}{2}u^2\right) + \frac{\partial}{\partial x}\rho u\left(e + \frac{p}{\rho} + \frac{1}{2}u^2\right) = Q + \frac{\partial}{\partial x}\left(k\frac{\partial T}{\partial x}\right) + \frac{\partial}{\partial x}\left[u\left(\frac{4}{3}\mu + \mu_v\right)\frac{\partial u}{\partial x}\right] \tag{5}$$

$$e = p/\rho(\gamma - 1) \tag{6}$$

By virtue of the assumed symmetry, only the region from $x = 0$ to $x = L$ is considered. Boundary conditions for these equations are $u = 0$ at $x = 0$ and $x = L$, $T = T_0$ at $x = L$, and $\partial T/\partial x = 0$ at $x = 0$.

The energy equation has a source term Q on the right side corresponding to fission-fragment heating. This volumetric heat source has the form

$$Q = Q_s h(t/t_D) L\frac{\partial}{\partial x} G\left(\frac{1}{L}\int_0^x \frac{\rho(x', t)}{\rho_0}\,dx'; S_H, S_F\right) = Q_s h(t/t_D)\left(\frac{\rho}{\rho_0}\right) G'\left(\frac{1}{L}\int_0^x \frac{\rho(x', t)}{\rho_0}\,dx'; S_H, S_F\right) \tag{7}$$

The quantity Q_s is the scale factor that converts the (nondimensional) neutron flux $h(t/t_D)$ into heating (kW/cm^3). The function h is the temporal variation of the neutron flux, which is approximately Gaussian, and t_D is the time scale characterizing the duration of the neutron pulse. The term $\partial G/\partial x$ is the spatial variation of the heating (see Fig. 2). The derivative $\partial/\partial x$ appears since the energy source term is the divergence of the nondimensional fission-fragment energy flux (G). The argument of G represents the coupling between the gas density field and fission-fragment energy deposition.[20,22–24] Since the absorption of fission-fragment energy depends on the number of absorbers (molecules) present per unit volume, the gas density appears in an integral in the argument of G, which is similar to its appearance in the related problem of light absorption by a gas. The function G is monotonically increasing with positive concavity, and the normalization of G is chosen conveniently to yield $G(0) = 0$ and $G(1) = 1$. Calculation of the x variation of Q from Eqs. (7) gives a roughly parabolic profile proportional to G', which is concave upward and has a minimum at $x = 0$. The quantities S_H and S_F are model-dependent similarity parameters[20] determining the precise form of the spatial variation of Q. As the homogeneity similarity parameter S_H is increased, the minimum for Q becomes deeper, and when $S_H = 0$, Q has no spatial variation. Thus, S_H is a measure of how homogeneous or spatially uniform the heating is. The foil-thickness similarity

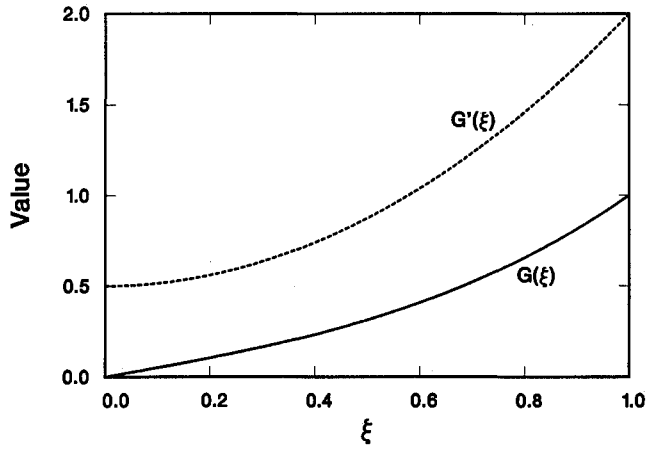

Fig. 2 Examples of $G(\xi)$ (solid) and $G'(\xi)$ (dashed).

parameter S_F has relatively little effect on the shape of Q and will not be discussed further. See Ref. 20 for a detailed discussion of Q.

There are several relevant timescales in this model: the time for an acoustic wave to travel from the side walls to the center; the time for thermal-conduction effects to reach the center from the side walls; the pulse duration; and the time required for the heating to increase the pressure and temperature by amounts comparable to their initial values. Typically, the acoustic timescale is much smaller than the other three timescales, so the Mach number of the induced flow is much less than unity. Therefore, the equations can be acoustically filtered.[20,25-26] This procedure has the effect of removing the wave nature of the pressure variation from the problem: the pressure partitions into a large mean $\bar{p}(t)$ plus a small local deviation $\hat{p}(x, t) = p(x, t) - \bar{p}(t)$. Thus, acoustic filtering effectively removes the acoustic time scale from consideration. The equations that result from this procedure are the following:

$$\frac{\partial \rho}{\partial t} + \frac{\partial}{\partial x}\rho u = 0 \tag{8}$$

$$\frac{\partial}{\partial t}\rho u + \frac{\partial}{\partial x}\rho u^2 = -\frac{\partial \hat{p}}{\partial x} + \frac{\partial}{\partial x}\left[\left(\frac{4}{3}\mu + \mu_v\right)\frac{\partial u}{\partial x}\right] \tag{9}$$

$$\frac{d\bar{p}}{dt} = (\gamma - 1)Q_s h(t/t_D) + \frac{(\gamma - 1)}{L}\left(k\frac{\partial T}{\partial x}\right)\bigg|_{x=L} \tag{10}$$

$$\gamma \bar{p} u = (\gamma - 1)Q_s h(t/t_D)L \times \left[G\left(\frac{1}{L}\int_0^x \frac{\rho(x', t)}{\rho_0}\,dx'\right) - \frac{x}{L}\right] + (\gamma - 1)\left[k\frac{\partial T}{\partial x} - \frac{x}{L}\left(k\frac{\partial T}{\partial x}\right)\bigg|_{x=L}\right] \tag{11}$$

$$\bar{p} = R\rho T \tag{12}$$

The general procedure to obtain these equations is outlined in Ref. 20 although the thermal-conduction and viscous terms are not included in that study.

These equations have the following physical interpretations. Equations (8) and (9) are just mass and momentum conservation [since $\bar{p}$ is not a function of x, it does not appear in Eq. (9)]. Equations (10) and (11) are related to energy conservation. Equation (10) shows that the mean pressure rise is governed by the mean heat addition minus the mean heat loss by thermal conduction (it is the perfect gas law in an unusual form). Equation (11) shows that velocities are induced when the local heating (both applied and conduction) differs from the mean heating [shown in Eq. (10)]. Thus, the tendency is for the system to approach uniform heating.[20] Note that $\hat{p}$ appears only in Eq. (9), so it decouples from the motion.

To assess different flow and heat transfer regimes, it is necessary to cast these equations in nondimensional form. The following nondimensionalization is used:

$$\tilde{\rho} = \rho/\rho_0 \qquad \tilde{p} = \bar{p}/p_0$$
$$\tilde{T} = T/T_0 \qquad \tilde{k} = k/k_0$$
$$\tilde{x} = x/L \qquad \tilde{t} = t/t_D$$
$$\tilde{u} = ut_D/L \qquad \tilde{\pi} = \hat{p}t_D^2/\rho_0 L^2(1 + S_B)$$
$$\tilde{\mu} = \mu/\mu_0 \qquad \tilde{\mu}_v = \mu_v/\mu_0$$

where S_B will be defined shortly. The equations that result from this procedure are

$$\tilde{p} = \tilde{\rho}\tilde{T} \tag{13}$$

$$\tilde{k} = \tilde{T}^{\alpha} \tag{14}$$

$$\frac{\partial \tilde{\rho}}{\partial \tilde{t}} + \frac{\partial}{\partial \tilde{x}}\tilde{\rho}\tilde{u} = 0 \tag{15}$$

$$S_A^{-1}\frac{d\tilde{p}}{d\tilde{t}} = h(\tilde{t}) + S_Q^{-1}\left(\tilde{k}\frac{\partial \tilde{T}}{\partial \tilde{x}}\right)\bigg|_{\tilde{x}=1} \tag{16}$$

$$S_A^{-1}\gamma\tilde{p}\tilde{u} = h(\tilde{t})\left[G\left(\int_0^{\tilde{x}}\tilde{\rho}\,d\tilde{x}'\right) - \tilde{x}\right] + S_Q^{-1}\left[\tilde{k}\frac{\partial \tilde{T}}{\partial \tilde{x}} - \tilde{x}\left(\tilde{k}\frac{\partial \tilde{T}}{\partial \tilde{x}}\right)\bigg|_{\tilde{x}=1}\right] \tag{17}$$

$$\frac{\partial}{\partial \tilde{t}}\tilde{\rho}\tilde{u} + \frac{\partial}{\partial \tilde{x}}\tilde{\rho}\tilde{u}^2 = -(1 + S_B)\frac{\partial \tilde{\pi}}{\partial \tilde{x}} + S_B\left(\frac{\mu_0 c_p}{\gamma k_0}\right)\frac{\partial}{\partial \tilde{x}}\left[\left(\frac{4}{3}\tilde{\mu} + \tilde{\mu}_v\right)\frac{\partial \tilde{u}}{\partial \tilde{x}}\right] \tag{18}$$

Here, the parameters S_A, S_Q, and S_B are defined as follows:

$$S_A = (\gamma - 1)Q_s t_D/p_0 \tag{19}$$

$$S_Q = Q_s L^2/k_0 T_0 \tag{20}$$

$$S_B = (\gamma - 1)k_0 T_0 t_D/p_0 L^2 \tag{21}$$

The amplitude similarity parameter S_A is the ratio of the pulse duration to the pressure-rise time scale and as such indicates the scale of the normalized pressure rise that would be produced by the heating in the absence of thermal conduction. The heating similarity parameter S_Q is proportional to the ratio of the thermal-conduction time scale (the time required for the thermal boundary layers to grow from the side walls into the center of the laser cell) to the pressure-rise time scale and, therefore, measures the relative strength of the applied heating to thermal-conduction loss. The boundary-layer similarity parameter S_B is proportional to the ratio of the pulse duration to the thermal-conduction time scale. Note that these parameters are not independent but obey the relation

$$S_A = S_B S_Q \tag{22}$$

Since in the notation of Carslaw and Jaeger[27] the thermal-conduction timescale t_C can be estimated using a value of $x/2\sqrt{\kappa t_C} \approx 2$ with $x = L$ and $\kappa = k_0/\rho_0 c_v$, the thermal-conduction time scale t_C and the pulse duration t_D are approximately equal when $S_B = S_B^* \approx 1/16$. Thus, S_B^* is the reference value to which S_B is to be compared to determine the relative importance of thermal-conduction and heating-nonuniformity effects.

The type of motion that results is governed by the relative values of these parameters. This behavior can be determined through application of the principle of dominant balance.[28] Simply put, the largest terms in these equations must be approximately equal, and smaller terms can be neglected. In both Eqs. (16) and (17) there are three terms: a source term involving h, a loss term involving thermal conduction scaled by S_Q^{-1}, and a dynamic-response term scaled by S_A^{-1}. Since this study emphasizes motion induced by the applied heating, the source term must be balanced by (at least) one of the other two terms. (By way of contrast, the cool-down period following the termination of heating is not considered herein.) Suppose $S_B/S_B^* \ll 1$. Then, by Eq. (22), terms proportional to S_A^{-1} are much larger than terms proportional to S_Q^{-1}, so the balance is between the source terms and the dynamic-

response terms. This is the negligible-conduction regime. Suppose $S_B/S_B^* >> 1$. Then, by Eq. (22), terms proportional to S_A^{-1} are much smaller than terms proportional to S_Q^{-1}, so the balance is between the source terms and the loss terms. This is the dominant-conduction regime. Suppose $S_B/S_B^* \sim 1$. Then, by Eq. (22), all terms are of the same magnitude, so no terms can be removed from the equations. This is the mixed regime.

Negligible-Conduction Regime

In the negligible-conduction regime ($S_B/S_B^* << 1$), thermal-conduction effects are confined to thin boundary layers at the side walls. The total heat removed from the gas by thermal conduction over the duration of the pulse is thus very small and does not affect the gas motion significantly. In the limit $S_B \to 0$, the equations have the following solution in Lagrangian parametric form[20]:

$$\tilde{p} = 1 + S_A \int_{-\infty}^{\tilde{t}} h(\tau)\mathrm{d}\tau \tag{23}$$

$$\tilde{\rho} = \{G'(\tilde{x}_0) + [1 - G'(\tilde{x}_0)]\tilde{p}^{-1/\gamma}\}^{-1} \tag{24}$$

$$\tilde{x} = G(\tilde{x}_0) + [\tilde{x} - G(\tilde{x}_0)]\tilde{p}^{-1/\gamma} \tag{25}$$

$$G'(\xi) = \mathrm{d}G/\mathrm{d}\xi \tag{26}$$

In these equations, the parametric variable $\tilde{x}_0$ must be eliminated to find the density field $\tilde{\rho}(\tilde{x}, \tilde{t})$. Although previously derived,[20] the solution for this regime is presented here to illustrate its region of validity ($S_B/S_B^* << 1$) and to contrast this regime with the other regimes. Note that S_A is the important similarity parameter in this regime.

From the above equations, it is seen that the gas density distribution at a given time is determined by the normalized pressure at that time, which is also the normalized amount of energy in the gas at that time [see Eq. (23)]. By way of contrast, the heating rate (proportional to h) is unimportant since it enters only in an integral sense in Eq. (23). Since the quantity $\tilde{x}_0 - G(\tilde{x}_0)$ is positive (see Fig. 2), the induced gas flow is inward and improves the heating uniformity (absorbers move into the low-flux region near $x = 0$ and out of the high-flux region near $x = L$). A density maximum is thus produced in the center, so the heated region is optically focusing. Note also that as $\tilde{p}$ (or equivalently S_A) becomes large, the density field approaches a limiting profile, which is unaffected by further heat addition. Analytical results for $\tilde{u}$, $\tilde{\pi}$, and other quantities are contained in the Appendix.

As an example, consider helium gas, initially at 200 kPa and 300 K, contained in a laser cell with a 1-cm gap (L = 0.5 cm) and with 1-μm UO_2 layers on the side walls. The heating is described by Q_s = 3.55 kW/cm^3 and h = 1 for $0 \le t \le t_D$ with t_D = 0.1 ms (h = 0 at other times). For this case, $S_B/S_B^* = 0.0095$. Figures 3–5 show the density, temperature, and applied heating fields, respectively, at 0.05 ms and 0.1 ms as determined from a numerical simulation of the full filtered equations using a finite difference method.[17] Outside the thin thermal boundary layers, the gas motion is inward, as discussed earlier. Also, the heating has become slightly more uniform at later times.

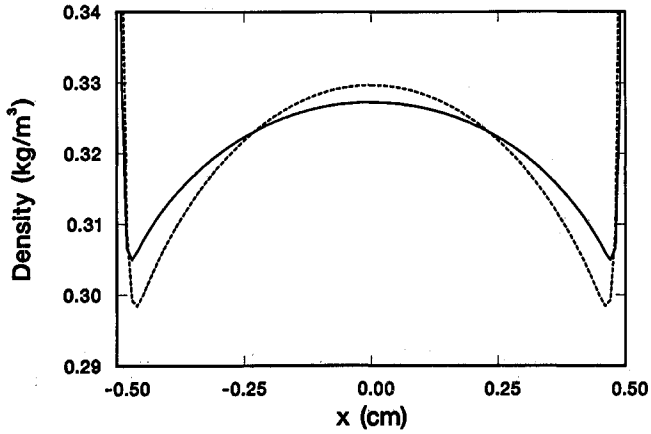

Fig. 3 Density at 0.05 ms (solid) and 0.1 ms (dashed).

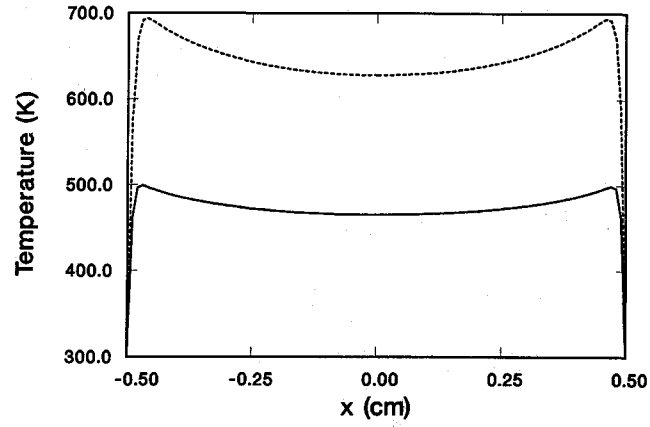

Fig. 4 Temperature at 0.05 ms (solid) and 0.1 ms (dashed).

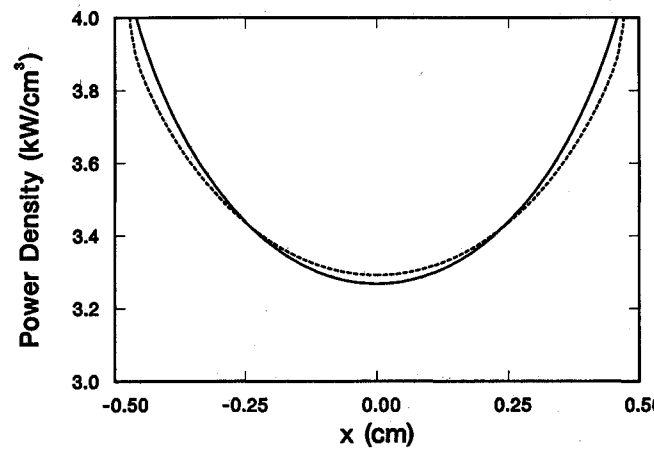

Fig. 5 Heating at 0.05 ms (solid) and 0.1 ms (dashed).

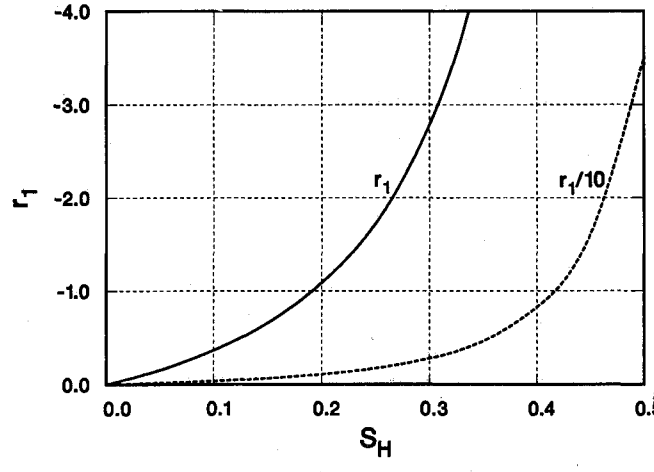

Fig. 6 Plot of r_1 vs S_H for S_F = 0.2 (dashed, 1/10 scale).

The quantity $\partial^2\tilde{\rho}/\partial\tilde{x}^2(0)$, often used in optical stability analyses of laser resonators,[13-15] can be determined for the negligible-conduction regime. In the limit $S_B \to 0$ with $\int_{-\infty}^{\infty} h(\tau)\mathrm{d}\tau = 1$, this quantity can be expressed as

$$\frac{\partial^2\tilde{\rho}}{\partial\tilde{x}^2}(0) = r_1(S_H, S_F)r_2(S_A, S_H, S_F) \tag{27}$$

Plots of r_1 and r_2 are given in Figs. 6 and 7. From these graphs,

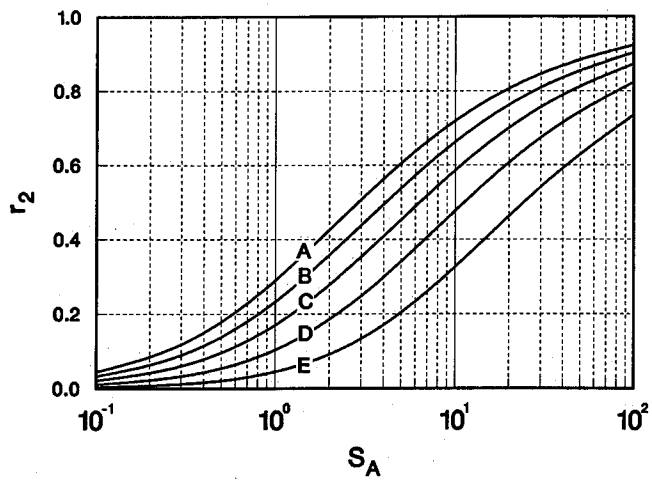

Fig. 7 Plot of r_2 vs S_A for $S_F = 0.2$ and $S_H = 0.1$ (A), 0.2 (B), 0.3 (C), 0.4 (D), 0.5 (E).

it is seen that large heating (large S_A) and large nonuniformity (large S_H) produce large curvature of the density field and thus strong focusing.

Several analyses of experiments have been reported involving conditions in the negligible-conduction regime.[13,15,19] Experimental data include pressure-rise and optical measurements, which permit determination of the pressure rise (energy deposition) at which the gas motion produces sufficient lensing to change the laser resonator from a stable to an unstable resonator (this stability transition is manifested as an abrupt change in the intensity of the emitted laser light). The dependence of the gas motion and, thus, the lensing on the energy deposition alone has been verified, and there is good quantitative agreement between model predictions of the density curvature and values inferred from the experiments.[13,15]

Dominant-Conduction Regime

In the dominant-conduction regime ($S_B S_B^* >> 1$), thermal conduction affects the gas flow everywhere and removes heat as rapidly as it is deposited. In the limit $S_B \to \infty$, the equations have the following solution in Lagrangian parametric form:

$$\tilde{p} = \int_0^1 \{1 + [H(1) - H(\xi)]\alpha S_Q h/\tilde{p}\}^{1/\alpha} d\xi \qquad (28)$$

$$\tilde{\rho} = \tilde{p}\{1 + [H(1) - H(\tilde{x}_0)]\alpha S_Q h/\tilde{p}\}^{-1/\alpha} \qquad (29)$$

$$\tilde{x} = \tilde{p}^{-1} \int_0^{\tilde{x}_0} \{1 + [H(1) - H(\xi)]\alpha S_Q h/\tilde{p}\}^{1/\alpha} \qquad (30)$$

$$H(\tilde{x}_0) = \int_0^{\tilde{x}_0} G(\xi) d\xi \qquad (31)$$

In these equations, the parametric variable $\tilde{x}_0$ must be eliminated to find the density field $\tilde{\rho}(\tilde{x}, \tilde{t})$. Also, Eq. (28) is an implicit equation for the pressure $\tilde{p}$. Note that S_Q is the important similarity parameter in this regime.

From Eqs. (28–31), it is seen that the gas density distribution at a given time is determined by the heating rate (proportional to h) at that time. By way of contrast, the amount of energy added to the gas up to that time (proportional to the time integral of h) is unimportant. Since H is monotonically increasing, Eq. (29) indicates that the gas density is smallest at the center and largest at the side walls, so the heated region is optically defocusing. Moreover, this minimum becomes deeper (outward flow) as h increases and shallower (inward flow) as h decreases. Thus, thermal-conduction effects actually worsen the heating nonuniformity by increasing the density near the wall (putting more absorbers in a high-flux region) and by decreasing the density near the center (removing absorbers from a low-flux region). Note also that, as $\tilde{p}$ (or equivalently S_Q) becomes large, the density field approaches a limiting profile, which is unaffected by further increasing the heat addition. Analytical results for $\tilde{u}$, $\tilde{\pi}$, and other quantities are contained in the Appendix.

As an example, consider helium gas, initially at 200 kPa and 300 K, contained in a laser cell with a 1-cm gap (L = 0.5 cm) and with 1-μm UO_2 layers on the side walls. The heating is described by $Q_s = 2.22 \times 10^{-3}$ kW/cm^3 and $h = 1$ for $0 \le t \le t_D$ with $t_D = 160$ ms ($h = 0$ at other times). For this case, $S_B/S_B^* = 15$. Figures 8–10 show the density, temperature, and applied heating fields, respectively, at 80

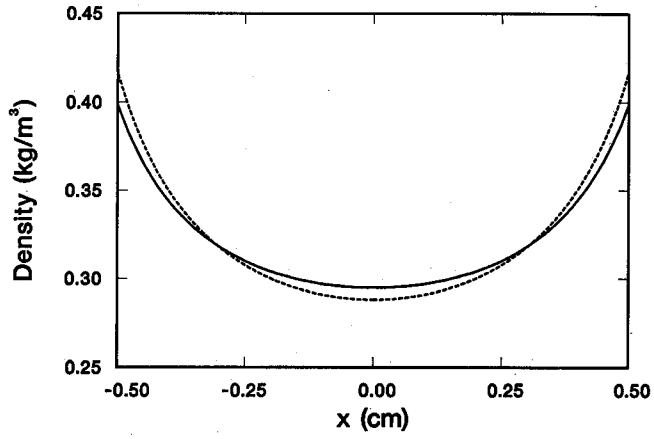

Fig. 8 Density at 80 ms (solid) and 160 ms (dashed).

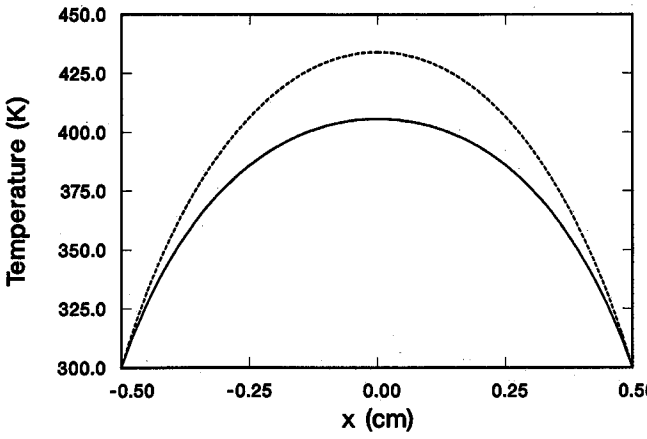

Fig. 9 Temperature at 80 ms (solid) and 160 ms (dashed).

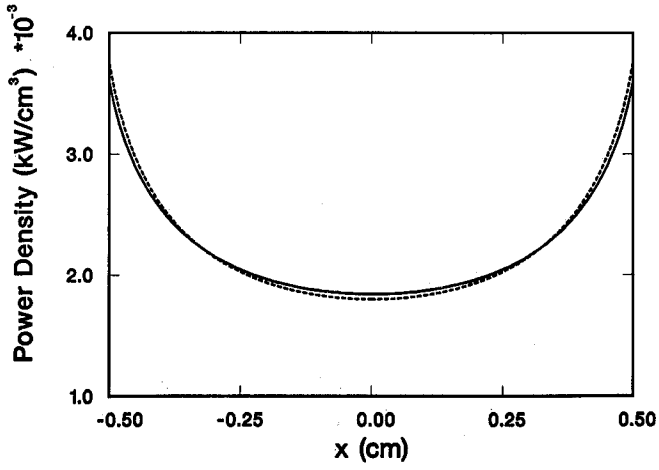

Fig. 10 Heating at 80 ms (solid) and 160 ms (dashed).

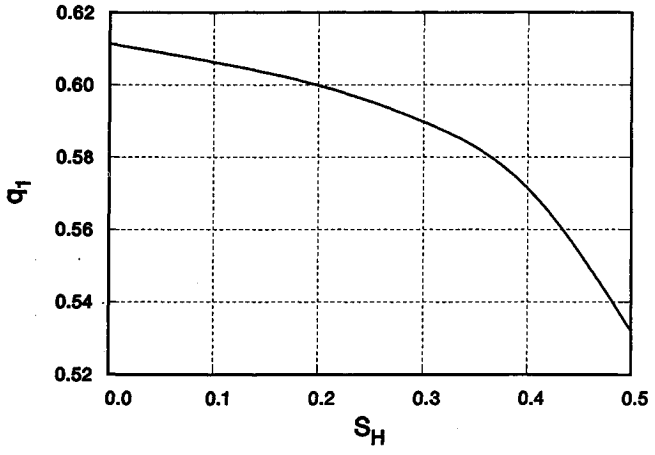

Fig. 11 Plot of q_1 vs S_H for $S_F = 0.2$ and $\alpha = 0.75$.

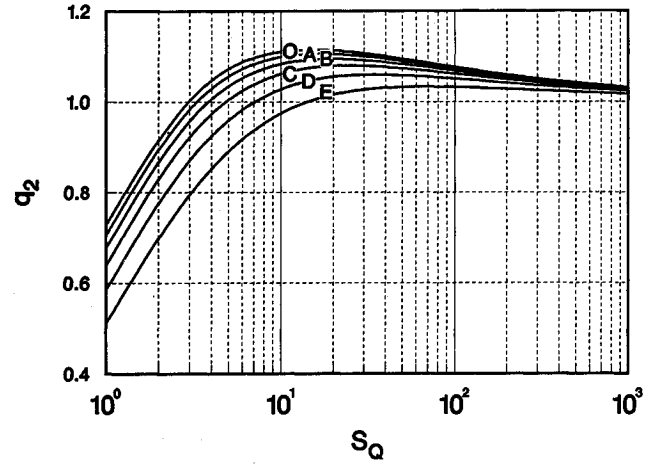

Fig. 12 Plot of q_2 vs S_Q for $S_F = 0.2$, $\alpha = 0.75$, and $S_H = 0.0$ (O), 0.1 (A), 0.2 (B), 0.3 (C), 0.4 (D), 0.5 (E).

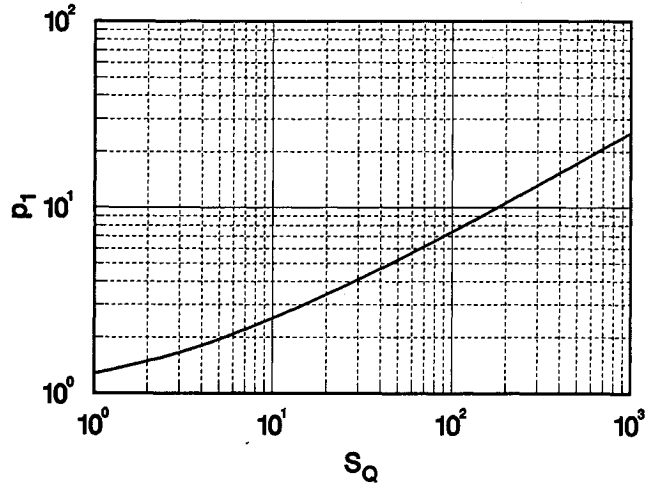

Fig. 13 Plot of p_1 vs S_H for $S_F = 0.2$ and $\alpha = 0.75$.

and 160 ms, as determined from a numerical simulation of the full filtered equations using a finite difference method.[17] Note that the density field does not vary significantly when the heating is held constant.

The quantity $\partial^2\tilde{\rho}/\partial\tilde{x}^2(0)$ can be determned for the dominant-conduction regime. In the limit $S_B \to \infty$ with $h(\tilde{t}) = 1$, this quantity can be expressed as

$$\frac{\partial^2\tilde{\rho}}{\partial\tilde{x}^2}(0) = q_1(S_H, S_F)q_2(S_Q, S_H, S_F) \tag{32}$$

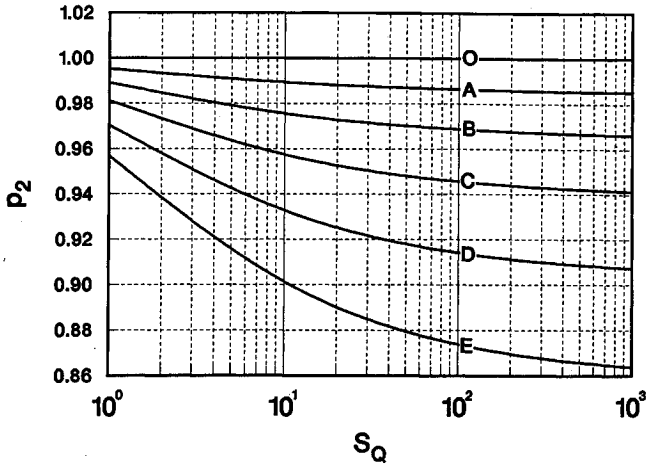

Fig. 14 Plot of p_2 vs S_Q for $S_F = 0.2$, $\alpha = 0.75$, and $S_H = 0.0$ (O), 0.1 (A), 0.2 (B), 0.3 (C), 0.4 (D), 0.5 (E).

Plots of q_1 and q_2 are given in Figs. 11 and 12. From these graphs, it is seen that the curvature does not depend strongly on S_H or S_Q for S_Q above unity.

The normalized pressure $\tilde{p}$ can also be determined for the dominant-conduction regime. In the limit $S_B \to \infty$ with $h(\tilde{t}) = 1$, this quantity can be expressed as

$$\tilde{p} = p_1(S_H, S_F)p_2(S_Q, S_H, S_F) \tag{33}$$

Plots of p_1 and p_2 are given in Figs. 13 and 14. From these graphs, it is seen that S_H does not affect $\tilde{p}$ greatly, but increasing S_Q (increasing the heating relative to the ability of thermal conduction to remove heat) is seen to increase $\tilde{p}$.

Mixed Regime

In the mixed regime ($S_B/S_B^* \sim 1$), the competing effects of spatially nonuniform heating and thermal conduction produce a complex gas motion. No analytical solution is available; however, qualitative statements can be made regarding the flow based on the results of the two previous sections. Since S_B/S_B^* is the ratio of the pulse duration to the thermal boundary-layer growth time, the thermal boundary layers are thin at early times but have reached the center of the laser cell at later times. Therefore, mixed cases resemble negligible-conduction cases at early times and dominant-conduction cases at later times. Similarly, the flow in the central region resembles the flow in the negligible-conduction regime, but the flow near the side walls resembles the flow in the dominant-conduction regime.Thus, the competition of thermal-conduction and heating-nonuniformity effects acts to produce both a density maximum at $x = 0$ and large densities at the side walls, with density minima at intermediate locations. These minima are quite close to the walls at early times, but they propagate in toward the center and eventualy engulf the central maximum. Furthermore, this motion depends in a complex manner on both the energy, as in the negligible-conduction regime, and the power, as in the dominant-conduction regime. Note that there are both optically focusing and defocusing regions since both maxima and minima exist in the density field.

As an example, consider helium gas, initially at 20 kPa and 300 K, contained in a laser cell with a 1-cm gap ($L = 0.5$ cm) and with 1-μm UO_2 layers on the side walls. The heating is described by $Q_s = 0.089$ kW/cm^3 and $h = 1$ for $0 \le t \le t_D$ with $t_D = 4$ ms ($h = 0$ at other times). For this case, $S_B/S_B^* = 0.38$. Figures 15–17 show the density, temperature, and applied heating fields, respectively, at 2 and 4 ms, as determined from a numerical simulation of the full filtered equations using a finite difference method.[17] For cases in the mixed regime, the flow is frequently observed to reduce the density in the central region but maintain a roughly constant density curvature in this region while doing so.

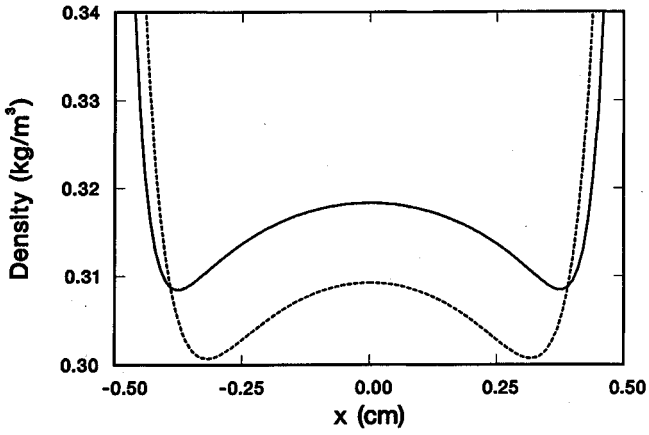

Fig. 15 Density at 2 ms (solid) and 4 ms (dashed).

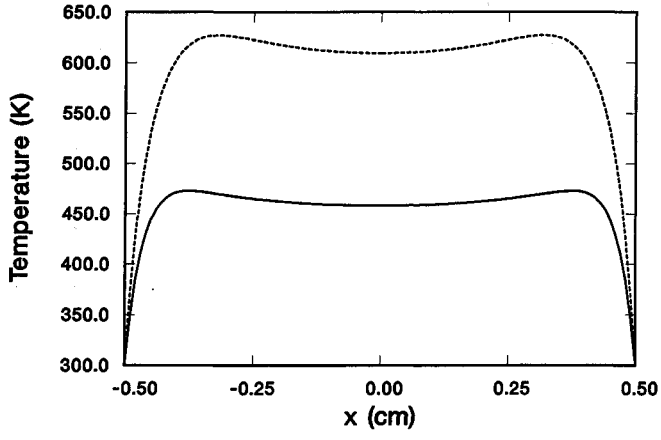

Fig. 16 Temperature at 2 ms (solid) and 4 ms (dashed).

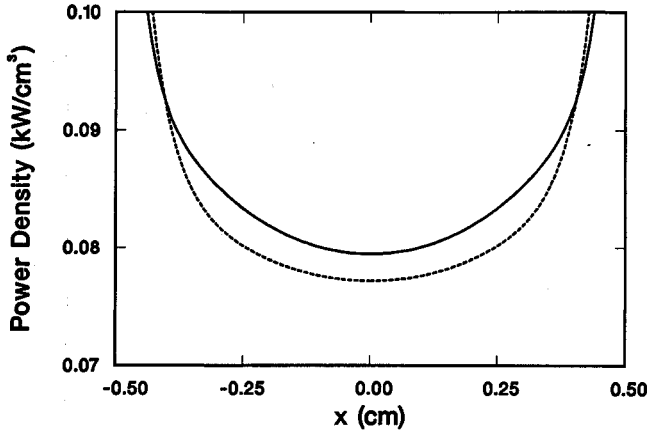

Fig. 17 Heating at 2 ms (solid) and 4 ms (dashed).

Conclusions

A model describing the gas flow in a nuclear-reactor-pumped laser has been examined. This gas flow is induced by the competition between the spatial nonuniformity of the fission-fragment heating and the effects of thermal conduction to the side walls. Three regimes are found and characterized in terms of S_B/S_B^*, the ratio of the pulse duration to the thermal boundary-layer growth time. The negligible-conduction regime corresponds to small values of S_B/S_B^*. In this regime, the density field is determined solely by the energy deposited in the gas (the power is unimportant), and a central density maximum is formed (an optically focusing region). Thermal-conduction effects are confined to thin boundary layers, and little heat is removed during the pulse. The dominant-conduction regime corresponds to large values of S_B/S_B^*. In this regime, the density field is determined solely by the power (rate of heating) in the gas (the energy deposited is unimportant), and a central density minimum is formed (an optically defocusing region). Thermal conduction removes heat as rapidly as it is deposited during the pulse. The mixed regime corresponds to values of S_B/S_B^* near unity. In this regime, the density field is determined by the energy and the power. At early times, a central density maximum forms, but density minima propagate inward from the side walls and ultimately engulf the central density maximum. It is often found that the curvature of the density field in the central region remains relatively constant during the latter portion of the pulse even though the density in the central region falls significantly. Analytical solutions of the equations were presented in the limits $S_B \to 0$ (negligible conduction) and $S_B \to \infty$ (dominant conduction). These solutions were used to generate graphs of the curvature of the density field in terms of the relevant dimensionless parameters.

The general behavior of the gas motion can be summarized by the following statement: gas flows away from the "hottest" regions and toward the "coldest" regions. The terms "hottest" and "coldest" in this context do not strictly refer to high or low temperature but rather to large or small total heating rate, where the total heating rate is the sum of the applied heating and the thermal-conduction loss and can be of either sign. In the negligible-conduction regime, thermal conduction is relatively unimportant, so the spatial variation of the applied heating alone determines the hottest and coldest spots. Since the applied heating is largest (hottest) near the side walls and smallest (coldest) in the center, gas flows away from the side walls and accumulates in the center. In the dominant-conduction regime, thermal conduction causes the coldness of the side walls, maintained at the initial gas temperature, to govern the gas motion everywhere. Thermal-conduction loss is most negative (coldest) in the region near the side walls and least negative (hottest) in the center, so gas flows from the latter to the former. In the mixed regime, the gas near the side walls is influenced primarily by their coldness and moves toward them, whereas the gas near the center experiences only the applied heating over the time of interest and flows inward since the center is the coldest point of the applied heating. This creates the w-shaped density profiles characteristic of this regime.

Appendix: Additional Analytical Results

This Appendix contains a compilation of analytical results relating to gas motion in the negligible-conduction and dominant-conduction regimes. Frequent use has been made of the equation of continuity written in Lagrangian form:

$$\tilde{\rho}\left(\frac{\partial \tilde{x}}{\partial \tilde{x}_0}\right)_t = 1 \tag{A1}$$

The following are analytical results for $\tilde{u}$, $\tilde{\pi}$, $\tilde{Q} = Q/Q_s$, and the density curvature in the limit $S_B \to 0$:

$$\tilde{u} = -\frac{S_A h}{\gamma \tilde{p}}\left[\tilde{x} - G(\tilde{x}_0)\right] \tag{A2}$$

$$\tilde{\pi} = \left\{-\frac{d^2}{d\tilde{t}^2}\tilde{p}^{\,1/\gamma}\right\}\left\{-(1-\tilde{p}^{\,1/\gamma})\int_0^1 [\xi - G(\xi)]^2 d\xi - \int_0^1 (1-\xi)[\xi - G(\xi)]d\xi + \int_0^{\tilde{x}_0} [\xi - G(\xi)]d\xi\right\} \tag{A3}$$

$$\tilde{Q} = hG'(\tilde{x}_0)\tilde{\rho} \tag{A4}$$

$$\frac{\partial^2\tilde{\rho}}{\partial\tilde{x}^2}(0) = -\frac{(1-\tilde{\rho}^{-1/\gamma})G'''(0)}{\{G'(0)+[1-G'(0)]\tilde{\rho}^{-1/\gamma}\}^4} \quad \text{(A5)}$$

Parametric expressions for the density field $\tilde{\rho}(\tilde{x})$ are given in the limit $S_A \to \infty$:

$$\tilde{\rho} \to [G'(\tilde{x}_0)]^{-1} \quad \text{(A6)}$$

$$\tilde{x} \to G(\tilde{x}_0) \quad \text{(A7)}$$

This limiting field is to be interpreted as a bound on the motion rather than as a physically realizable field.

The following are analytical results for $\tilde{u}$, $\tilde{\pi}$, $\tilde{Q} = Q/Q_s$, and the density curvature in the limit $S_B \to \infty$:

$$\tilde{u} = \left\{\frac{S_Q}{\tilde{\rho}^2}\frac{dh}{d\tilde{t}}\right\}\left\{I(\tilde{x}_0) - I(1)\left[\frac{\tilde{\rho}^2\tilde{x}+hI(\tilde{x}_0)}{\tilde{\rho}^2+hI(1)}\right]\right\} \quad \text{(A8a)}$$

$$I(\tilde{x}_0) = \int_0^{\tilde{x}_0}\{1+[H(1)-H(\xi)]\alpha S_Q h/\tilde{\rho}\}^{-1+1/\alpha} \times [H(1)-H(\xi)]\mathrm{d}\xi \quad \text{(A8b)}$$

$$\tilde{\pi} = \left(\frac{\mu_0 c_p}{\gamma k_0}\right)\left(\frac{4}{3}\tilde{\mu}+\tilde{\mu}_v\right) \times \left\{\tilde{\rho}J(\tilde{x}_0) - I(1)\left[\frac{\tilde{\rho}^2+h\tilde{\rho}J(\tilde{x}_0)}{\tilde{\rho}^2+hI(1)}\right]\right\} \quad \text{(A9a)}$$

$$J(\tilde{x}_0) = \{1+[H(1)-H(\tilde{x}_0)]\alpha S_Q h/\tilde{\rho}\}^{-1+1/\alpha} \times [H(1)-H(\tilde{x}_0)] \quad \text{(A9b)}$$

$$\tilde{Q} = hG'(\tilde{x}_0)\tilde{\rho} \quad \text{(A10)}$$

$$\frac{\partial^2\tilde{\rho}}{\partial\tilde{x}^2}(0) = \frac{S_Q h\tilde{\rho}^2 G'(0)}{[1+H(1)\alpha S_Q h/\tilde{\rho}]^{1+3/\alpha}} \quad \text{(A11)}$$

Parametric expressions for the density field $\tilde{\rho}(\tilde{x})$ in the limit $S_Q \to \infty$:

$$\tilde{\rho} \to \frac{\int_0^1 [H(1)-H(\xi)]^{1/\alpha}\mathrm{d}\xi}{[H(1)-H(\tilde{x}_0)]^{1/\alpha}} \quad \text{(A12)}$$

$$\tilde{x} \to \frac{\int_0^{\tilde{x}_0}[H(1)-H(\xi)]^{1/\alpha}\mathrm{d}\xi}{\int_0^1[H(1)-H(\xi)]^{1/\alpha}\mathrm{d}\xi} \quad \text{(A13)}$$

This limiting field is to be interpreted as a bound on the motion rather than as a physically realizable field. Note that this density field has an integrable singularity at $\tilde{x} = \tilde{x}_0 = 1$.

Acknowledgment

This work was performed at Sandia National Laboratories, supported by the U.S. Department of Energy under Contract DE-AC04-76DP00789.

References

[1]Thom, K., and Schneider, R. T., "Nuclear Pumped Gas Lasers," *AIAA Journal*, Vol. 10, No. 4, 1972, pp. 400–406.

[2]McArthur, D. A., and Tollefsrud, P. B., "Observation of Laser Action in CO Gas Excited Only by Fission Fragments," *Applied Physics Letters*, Vol. 26, Feb. 1975, pp. 187–190.

[3]Helmick, H. H., Fuller, J. L., and Schneider, R. T., "Direct Nuclear Pumping of a Helium-Xenon Laser," *Applied Physics Letters*, Vol. 26, March 1975, pp. 327–328.

[4]Miley, G. H., "Direct Nuclear Pumped Lasers—Status and Potential Applications," *Laser Interaction and Related Plasma Phenomena*, Vol. 4, edited by H. Hora and G. Miley, Plenum, New York, 1976, pp. 181–228.

[5]Prelas, M. A., Akerman, M. A., Boody, F. P., and Miley, G. H., "A Direct Nuclear Pumped 1.45-μ Atomic Carbon Laser in Mixtures of He-CO and He-CO_2," *Applied Physics Letters*, Vol. 31, Oct. 1977, pp. 428–430.

[6]De Young, R. J., Shiu, Y. J., and Williams, M. D., "Fission-Fragment Nuclear Lasing of Ar(He)-Xe," *Applied Physics Letters*, Vol. 37, Oct. 1980, pp. 679–681.

[7]Voinov, A. M., Dovbysh, L. E., Krivonosov, V. N., Mel'nikov, S. P., Podmoshenskii, I. V., and Sinyanskii, A. A., "Fission-Pumped He-Xe and Ar-Xe Infrared Lasers," *Soviet Technical Physics Letters*, Vol. 7, Aug. 1981, p. 437.

[8]Hays, G. N., McArthur, D. A., Neal, D. R., and Rice, J. K., "Gain Measurements Near 351 nm in ^{3}He/Xe/NF_3 Mixtures Excited by Fragments from the ^{3}He(n,p)^{3}H Reaction," *Applied Physics Letters*, Vol. 49, Aug. 1986, pp. 363–365.

[9]Rice, J. K., Hays, G. N., Neal, D. R., McArthur, D. A., and Alford, W. J., "Nuclear Reactor Excitation of XeF Laser Gas Mixtures," *Proceedings of the International Conference on Lasers '86*, edited by R. W. McMillan, STS Press, McLean, VA, 1987, pp. 571–578.

[10]McArthur, D. A., Hays, G. N., Alford, W. J., Neal, D. R., Bodette, D. E., and Rice, J. K., "Recent Results on Reactor-Pumped Laser Studies at Sandia National Laboratories," *Laser Interaction and Related Plasma Phenomena*, Vol. 8, edited by H. Hora and G. Miley, Plenum, New York, 1988, pp. 75–86.

[11]Miley, G. H., *Direct Conversion of Nuclear Radiation Energy*, 1st ed., American Nuclear Society, LaGrange, IL, 1970, Chaps. 3–4.

[12]Born, M., and Wolf, E., *Principles of Optics*, 6th ed., Pergamon, New York, 1980, pp. 87–98.

[13]Torczynski, J. R., and Neal, D. R., "Effect of Gasdynamics on Resonator Stability in Reactor-Pumped Lasers," Sandia National Laboratories, Albuquerque, NM, SAND88-1318, July 1988.

[14]Neal, D. R., Sweatt, W. C., and Torczynski, J. R., "Resonator Design with an Intracavity Time-Varying Index Gradient," *Current Developments in Optical Engineering III*, edited by R. E. Fischer and W. J. Smith, International Society for Optical Engineering, Vol. 965, 1989, pp. 130–141.

[15]Neal, D. R., Torczynski, J. R., and Sweatt, W. C., "Resonator Stability Effects in "Quadratic-Duct" Nuclear-Reactor-Pumped Lasers," *Proceedings of the International Conference Lasers '88*, edited by R. C. Sze and F. J. Duarte, STS Press, McLean VA, 1989, pp. 245–252.

[16]Torczynski, J. R., and Gross, R. J., "Refractive Index Gradients in Nuclear-Reactor-Pumped Lasers: Gasdynamic Effects," *Proceedings of the International Conference on Lasers '87*, edited by F. Duarte, STS Press, McLean, VA, 1988, pp. 241–248.

[17]Torczynski, J. R., and Gross, R. J., "The Gasdynamics of Fission-Fragment Heating," *Proceedings of the 1st National Fluid Dynamics Congress*, edited by C. Dalton, AIAA, Washington, DC, 1988, pp. 1040–1047.

[18]Torczynski, J. R., and Gross, R. J., "Axis-Shielding in Cylindrical Nuclear-Reactor-Pumped Lasers," *Journal of Applied Physics*, Vol. 64, Nov. 1988, pp. 4323–4328.

[19]Torczynski, J. R., Gross, R. J., Hays, G. N., Harms, G. A., Neal, D. R., McArthur, D. A., and Alford, W. J., "Fission-Fragment Energy Deposition in Argon," *Nuclear Science and Engineering*, Vol. 101, March 1989, pp. 280–284.

[20]Torczynski, J. R., "On the Motion of a Gas Experiencing Range-Dependent Volumetric Heating," *Journal of Fluid Mechanics*, Vol. 201, April 1989, pp. 167–188.

[21]Reid, R. C., Prausnitz, J. M., and Poling, B. C., *The Properties of Gases and Liquids*, 4th ed., McGraw-Hill, New York, 1986, pp. 514–518, 530, 531.

[22]Miley, G. H., and Thiess, P. E., "A Unified Approach to Two-Region Ionization-Excitation Density Calculations," *Nuclear Applications*, Vol. 6, May 1969, pp. 434–451.

[23]Guyot, J. C., Miley, G. H., and Verdeyen, J. T., "Application of a Two-Region Heavy Charged Particle Model to Noble-Gas Plasmas Induced by Nuclear Radiations," *Nuclear Science and Engineering*, Vol. 48, Aug. 1972, pp. 373–386.

[24]Chung, A. K., and Prelas, M. A., "The Transport of Heavy Charged Particles in a Cylindrical Nuclear-Pumped Plasma," *Nuclear Science and Engineering*, Vol. 86, March 1984, pp. 267–274.

[25]Rehm, R. G., and Baum, H. R., "The Equations of Motion for

Thermally Driven, Buoyant Flows," *Journal of Research of the National Bureau of Standards*, Vol. 83, May–June 1978, pp. 297–308.

[26]Paolucci, S., "On the Filtering of Sound from the Navier-Stokes Equations," Sandia National Laboratories, Albuquerque, NM, SAND82-8257, Dec. 1982.

[27]Carslaw, H. S., and Jaeger, J. C., *Conduction of Heat in Solids*, 2nd ed., Oxford, New York, 1986, p. 61.

[28]Bender, C. M., and Orszag, S. A., *Advanced Mathematical Methods for Scientists and Engineers*, 1st ed., McGraw-Hill, New York, 1978, pp. 83–88.